ROC Analysis Improves $CMRO_2$ Estimation for Rehabilitation Subjects

C. B. Glielmi[1], R. A. Schuchard[2], S. Laconte[1], and X. P. Hu[1]

[1]Department of Biomedical Engineering, Georgia Institute of Technology / Emory University, Atlanta, GA, United States, [2]Rehabilitation Research & Development Center, VA Medical Center, Atlanta, GA, United States

INTRODUCTION Longitudinal rehabilitation studies require fMRI measures and analysis techniques that provide consistency between scanning sessions. Cerebral blood flow (CBF) measurement and cerebral metabolic rate of oxygen ($CMRO_2$) estimation are considered to be more specific imaging markers of neuronal activity than blood-oxygenation level dependent (BOLD) contrast and more consistent between subjects and scanning sessions [1-3]. The vast majority of studies employing these metrics utilize animals or the healthy human population using several acquisition approaches which include optimized CBF acquisition in conjunction with either optimized BOLD contrast or "sub-optimal BOLD," the latter of which is a byproduct of CBF acquisition. As we prepare to expand CBF and $CMRO_2$ imaging to the rehabilitation patient population, we are exploring the reliability of sub-optimal BOLD/CBF to estimate $CMRO_2$ over the duration of rehabilitation. This work strives to quantitatively evaluate sub-optimal BOLD scans using receiver operator characteristics (ROC) analysis and demonstrates its ability to optimize $CMRO_2$ estimation. Specifically, we hypothesize that a) utilization of sub-optimal BOLD datasets with the highest ROC detectability will most consistently yield reasonable $CMRO_2$ estimates and b) selection of significance threshold at the "knee" of the ROC curve to determine region of interest (ROI) will optimize $CMRO_2$ estimation.

METHODS

Subjects and Image Acquisition: We conducted a multi-session monocular study for 2 subjects with retinitis pigmentosa (RP) acquiring optimal BOLD on one day and CBF/sub-optimal BOLD on a second day using a 3T Siemens scanner. For optimal BOLD, subjects were scanned using a block design (alternating 16 second blocks of rest and stimulation) with four types of stimuli (2 rings and 2 checkerboards at varied eccentricities and resolutions, respectively) presented to each subject's left eye (20/90 and 20/110 spatial acuity and 10 degrees radial visual field eccentricity). A single-shot gradient-echo EPI sequence was used to acquire T2*-weighted images over 33 oblique axial slices with TR/TE of 2000/30 ms, matrix of 64x64, FOV 22x22 and slice thickness of 3mm with no gap. Each scanning session consisted of 3 and 4 scans with checkerboard and ring stimulation, respectively. CBF/sub-optimal BOLD data were also acquired using a block design (48 seconds fixation followed by 48 seconds stimulus) with the same 4 types of stimuli. Sixteen axial slices (6mm-thick, 1.5mm gap) were acquired using a continuous arterial spin labeling (CASL) sequence with parameters of TR = 3s (effective TR = 6s), labeling duration = 1.4s, post-labeling delay = .7s, TE = 19ms, FOV = 20cm, matrix = 64X64, flip angle = 90° and acquisition = 112 and 144 volumes for ring and checkerboard scans, respectively [4]. Prior to statistical analysis, subtraction of control minus labeled images yields perfusion contrast and addition of control plus labeled images yields BOLD contrast. However, the relatively short TE required for optimized CBF contrast results in sub-optimal BOLD contrast. Assuming a range of BOLD calibration parameters, $CMRO_2$ was then estimated using the common simplified model [5]. All BOLD (optimal and sub-optimal) data were corrected for motion, slice scan time and linear drift removal and all CBF data were corrected for motion and slice scan time, as well as being smoothed with a 6 mm kernel.

ROC Analysis: True positives were first estimated by analyzing optimal BOLD data using SPM2's multi-run general linear model (GLM) at a high confidence level ($p<.05$ corrected for false discovery rate). Individual sub-optimal BOLD datasets were then analyzed using a GLM and compared to the reference activation map to calculate true positive fraction (TPF) and false positive fraction (FPF) at various levels of significance for each scan [6]. Detectability, estimated by the integral of the ROC curve, was then calculated to measure the performance of the procedure for each fMRI scan and stimulus. Subsequently, $CMRO_2$ estimates for each sub-optimal BOLD dataset were related to a) detectability and b) the ROC slope at various significance levels (which determine ROI used for estimation). Generally, the "knee" (ROC curve slope=1) yields the best balance between TPF and FPF.

	Number of Scans Within Range (Out of 8)		%ΔCMRO2 for scan with highest detectability (avg. of two subjects)	
m	Small Ring	Large Ring	Small Ring	Large Ring
0.5	1	0	24.1	10.2
1	3	2	27.6	25.2
1.5	3	4	34.1	-26.7
2	1	1	29.4	-5.5
2.5	1	0	-12.9	451.9

	Number of Scans Within Range (Out of 6)		%ΔCMRO2 for scan with highest detectability (avg. of two subjects)	
m	Checkerboard 1 (Low Resolution)	Checkerboard 1 (High Resolution)	Checkerboard 1 (Low Resolution)	Checkerboard 1 (High Resolution)
0.5	1	0	3.9	-9.3
1	4	4	14.2	6.8
1.5	1	2	13.4	19.8
2	2	1	29.5	267.2
2.5	1	0	147.2	1260.9

Table 1: For ring and checkerboard stimuli, ROC slope (m) of 1 yields $CMRO_2$ estimates within range more frequently than other slopes. Furthermore, for scans with highest detectability, the $\%\Delta CMRO_2$ (averaged between subjects for each stimulus) are within range for all stimuli at the ROC "knee."

RESULTS AND DISCUSSION We first determined a reasonable range of $\%\Delta CMRO_2$ (between 5 and 30% based on published values for similar stimuli) to evaluate $CMRO_2$ estimates [7]. Next, considering a range of points along the ROC curves we found that the highest proportion of datasets yielded $CMRO_2$ estimates within the reasonable range at the ROC "knee" (Table 1). For each subject and stimulus the dataset with the highest detectability yielded $CMRO_2$ estimates within range for all stimuli at the "knee" while estimates using other ROC significance levels were less commonly within range. Furthermore, estimates produced using the "knee" exhibited slightly higher $\%\Delta CMRO_2$ for the small ring and low resolution checkerboard relative to the large ring and high resolution checkerboard, respectively, which is consistent with the limited spatial acuities and eccentricities of the subjects. Commonly, ROC curves for a given subject and stimulus showed various detectabilities, the highest of which yielded the most reasonable $CMRO_2$ estimate. For example, three datasets for the low resolution checkerboard demonstrate various ROC performances, the highest of which (red curve, Fig 1A) yields $CMRO_2$ estimates within the expected range (yellow band) across a range of calibration parameters (Fig. 1B). Furthermore, the dataset with the highest detectability yields the most reliable $CMRO_2$ estimate when the "knee" is used relative to significance levels at other points along the ROC curve (Fig. 1C).

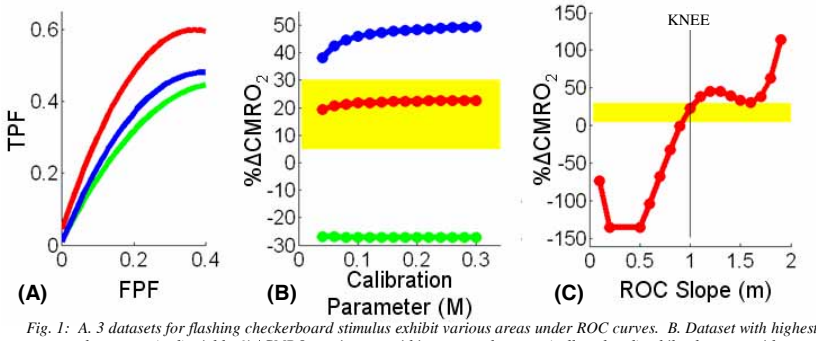

Fig. 1: A. 3 datasets for flashing checkerboard stimulus exhibit various areas under ROC curves. B. Dataset with highest area under curve (red) yields $\%\Delta CMRO_2$ estimates within expected range (yellow band) while datasets with poor detectability (blue and green) yield unreasonable estimates. C. $\%\Delta CMRO_2$ at various ROC slopes for dataset with highest detectability demonstrate that significance level at the "knee" yields estimate within expected range (yellow band).

CONCLUSION This study demonstrates that ROC analysis can optimize $CMRO_2$ estimation by enabling a) dataset selection based on detectability and b) significance threshold selection based on ROC slope. Optimizing $\%\Delta CMRO_2$ estimates despite sub-optimal BOLD acquisition provides great potential in rehabilitation studies beyond the scope of the low vision study presented in this work.

ACKNOWLEDGEMENTS This work was supported in part by the NIH RO1 EB002009 and the VA Rehabilitation R&D Service.

REFERENCES [1] Tjandra T, Brooks JCW, Figueiredo P, Wise R, Matthews PM, Tracy I. *NeuroImage* 2005;27:393-401. [2]Wong EC. *Functional MRI* 1999;63–9. [3] Sicard KM, Duong TQ. *NeuroImage* 2005;25:850-8. [4] Alsop DC, Detre JA. *Radiology* 1998;208:410-416. [5] Davis TL, Kwong KK, Weiskoff RM, Rosen BR. *Proc Natl Acad Sci USA* 1998 Feb 17;95(4):1834-9. [6]Tuong HL, Hu X. *NMR in Biomedicine* 1997;Vol. 10, 160-4. [7] Ulugdag K, Dubowitz DJ, Yoder EJ, Restom K, Liu TT, Buxton RB. *NeuroImage* 2004.;23:148-55.